Pharmaceutical Sciences and Drug Design
ISSN: 3062-4428
2024, Volume 4, Page No: 63-81

Available online at: www.galaxypub.co/page/journals

Galaxy Publication

Galaxy Publication

Network Pharmacology-Guided and Experimental Insights into the Therapeutic Effects of Sancao Yuyang Decoction on Oral Mucositis

Arun Prakash[1]*, Neha Desai[1]

[1]Department of Biotechnology, Faculty of Science, Delhi University, New Delhi, India.

***E-mail** ✉ arun.prakash.in@hotmail.com

Received: 19 February 2024; **Revised:** 21 May 2024; **Accepted:** 28 May 2024

ABSTRACT

This study aimed to elucidate the therapeutic mechanisms of Sancao Yuyang Decoction (SCYYD) in managing oral mucositis (OM) through a combination of computational and experimental approaches.Bioactive compounds in SCYYD and their potential molecular targets, along with OM-associated targets, were collected from public databases. Protein–protein interaction (PPI) networks, Gene Ontology (GO), and KEGG pathway analyses were employed to identify core targets and signaling pathways involved in SCYYD's effects. Networks linking ingredients, targets, and disease pathways were constructed. Molecular docking simulations were performed to evaluate the interactions between major compounds and key protein targets. The predictions were further validated using in vivo experiments in OM rat models.A total of 119 active compounds and 186 putative targets were identified. Bioinformatic analyses highlighted five principal compounds and ten core protein targets. GO and KEGG enrichment analyses suggested that SCYYD modulates multiple biological pathways, including HIF-1 and Ras signaling, to exert therapeutic effects. Molecular docking confirmed strong binding affinities of the main compounds to critical targets. In vivo studies demonstrated that SCYYD reduced inflammatory markers, accelerated mucosal healing, decreased the expression of SRC, HSP90AA1, STAT3, HIF1α, mTOR, TLR4, and MMP9, and increased ESR1 levels in OM rats.This integrative study reveals that SCYYD acts through multiple compounds and targets to mitigate OM, combining computational predictions with experimental evidence, and provides mechanistic insights for its pharmacological application.

Keywords: Oral mucositis, Sancao yuyang decoction, Multi-target therapy, Network pharmacology, Molecular docking, In vivo validation

How to Cite This Article: Prakash A, Desai N. Network Pharmacology-Guided and Experimental Insights into the Therapeutic Effects of Sancao Yuyang Decoction on Oral Mucositis. Pharm Sci Drug Des. 2024;4:63-81. https://doi.org/10.51847/Ey0Zr9qcrb

Introduction

Oral mucositis (OM) is characterized by inflammatory and/or ulcerative lesions of the oral mucosa, which can arise from various factors including infections, immune dysfunction, and certain medications [1]. It is a frequent complication among cancer patients undergoing radiotherapy and chemotherapy, with an incidence ranging from 40% to 70% [2, 3]. According to the ESMO mucositis guidelines, OM refers to mucosal inflammation induced by ionizing radiation or chemotherapeutic agents such as methotrexate, cyclophosphamide, and 5-fluorouracil (5-FU) [1]. Clinically, OM presents as erythema, erosion, and ulcerative lesions accompanied by severe pain, which can significantly impair eating, speaking, and sleeping [4]. The resulting nutritional deficits due to pain can further compromise overall health and quality of life in affected patients [5].

Current management strategies for OM include standardized oral care, antibiotics, anti-inflammatory agents, growth factors, analgesics, and various mouthwashes [6]. Although medications such as dexamethasone, cydiodine, and doxepin are commonly used to alleviate inflammation and pain, their prolonged use may lead to adverse effects including fungal infections, rashes, drowsiness, burning sensations, and fatigue [1, 7]. Consequently, there is an urgent need to develop effective therapeutic options for OM with minimal side effects.

Traditional Chinese medicine (TCM) has been employed in China for over 2000 years for disease prevention and treatment. In recent years, TCM has gained attention among OM patients due to its therapeutic efficacy and

favorable safety profile [8, 9]. Several herbal medicines with anti-inflammatory, antioxidant, and analgesic properties have shown promise in alleviating OM symptoms [10, 11]. Sancao Yuyang Decoction (SCYYD), a patented Chinese medicine formulation (Patent No. ZL 201810411853.2), comprises Lithospermum erythrorhizon (Zi Cao), Prunellae Spica (Xia Ku Cao), Menthae Herba (Bo He), and Licorice (Gan Cao). Clinical studies have demonstrated that SCYYD can reduce local inflammation and improve manifestations such as erythema, erosion, and oral ulcers in OM patients [12]. However, the underlying mechanisms of SCYYD in treating OM remain incompletely understood, warranting further investigation.

TCM formulations contain numerous bioactive components that may act synergistically through multiple mechanisms. The complexity of TCM necessitates systematic approaches to elucidate the interactions between individual components and their molecular targets. Network pharmacology, which integrates chemical informatics, bioinformatics, network biology, and pharmacology, offers a holistic framework to investigate multi-component, multi-target interactions [13, 14]. In this study, we combined network pharmacology analysis with in vivo validation to predict and verify the active ingredients of SCYYD, their protein targets, and the molecular mechanisms through which they act against OM. The detailed workflow of the study is illustrated in **Figure 1**.

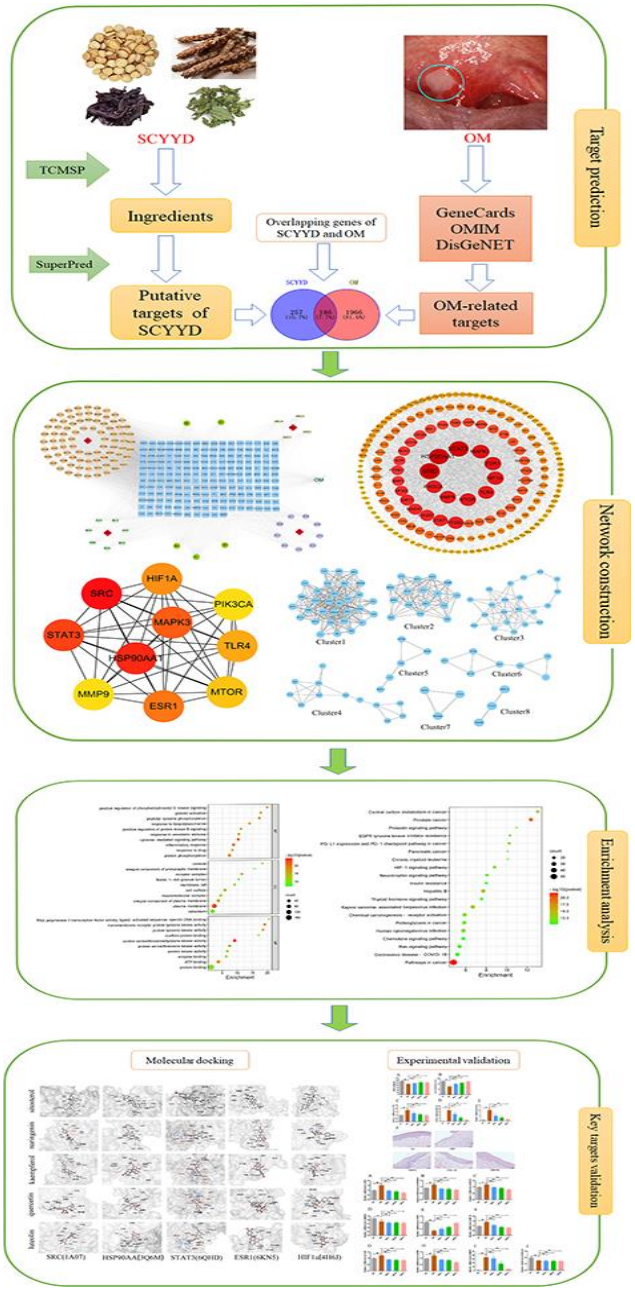

Figure 1. Detailed workflow of present study

Materials and Methods

Screening of active ingredients in SCYYD and prediction of their targets

The chemical constituents of Sancao Yuyang Decoction (SCYYD) were retrieved from the Traditional Chinese Medicine Systems Pharmacology Database and Analysis Platform (TCMSP, http://tcmspw.com/tcmsp.php). Oral bioavailability (OB) and drug-likeness (DL) were applied as criteria to evaluate ADME properties, with thresholds set at OB ≥30% and DL ≥0.18. Potential molecular targets of the identified active ingredients were predicted using the SuperPred database (https://prediction.charite.de/).

Identification of OM-related targets

Targets associated with oral mucositis (OM) were collected from GeneCards (https://www.genecards.org/), OMIM (https://omim.org/), and DisGeNET (https://www.disgenet.org/). The keyword “oral mucositis” was used, and duplicate entries were removed to obtain unique OM-related targets.

Construction of Ingredient–Target–Disease network

The overlapping targets between SCYYD and OM were identified using a Venn diagram, representing potential therapeutic targets. Cytoscape 3.8.2 software was employed to visualize the ingredient–target–disease network.

Protein–Protein Interaction (PPI) network analysis

The intersecting targets were uploaded to the STRING database (http://string-db.org) to construct the PPI network, setting the organism as *Homo sapiens* and a minimum interaction score of 0.7. Cytoscape 3.8.2, along with the Cytohubba and MCODE plugins, were used to identify core proteins and functional clusters. Biological processes of each cluster were further analyzed using DAVID Bioinformatics Resources 6.7 (http://david.abcc.ncifcrf.gov/).

GO and KEGG pathway enrichment analysis

Functional enrichment of the target genes was performed using DAVID for Gene Ontology (GO) and Kyoto Encyclopedia of Genes and Genomes (KEGG) pathway analysis. GO analysis included biological process (BP), cellular component (CC), and molecular function (MF) categories. Significance thresholds were set at $P<0.05$ and FDR<0.05. Cytoscape 3.8.2 was used to visualize the target–pathway network.

Molecular docking

Molecular docking was conducted to evaluate the binding affinity between key active ingredients and core protein targets. Structures of active compounds were downloaded in SDF format from PubChem (http://pubchem.ncbi.nlm.nih.gov), converted to mol2 format, and energy-minimized using Chem3D. Protein structures were obtained from the RCSB PDB database (https://www.rcsb.org/). Docking simulations were performed using CB-Dock2 (https://cadd.labshare.cn/cb-dock2/), where lower Vina scores indicate more stable ligand–protein interactions.

Preparation of SCYYD aqueous extract

The four component herbs of SCYYD—Lithospermum erythrorhizon, Prunellae Spica, Menthae Herba, and Licorice—were obtained from the pharmacy of Hangzhou Third People’s Hospital (Hangzhou, China) and mixed in a ratio of 2.5:5:1:5 (w/w). The mixture was soaked in distilled water (1:5, w/v) for 1 h, decocted twice for 30 min each, and concentrated to 1.825 g/mL, then stored at −20°C.

Animals and experimental design

Forty male Sprague-Dawley rats (180–200 g) were obtained from Shanghai Slac Laboratory Animal Co. Ltd. and housed in SPF conditions at the Laboratory Animal Research Center of Zhejiang Chinese Medical University (Hangzhou, China). Rats were maintained under standard laboratory conditions (23 ± 2°C, 50 ± 10% humidity, 12 h light/dark cycle) with ad libitum access to food and water. All procedures were approved by the Laboratory Animal Management and Ethics Committee of Zhejiang Chinese Medical University (Approval No. IACUC-20210503-08) and performed according to national regulations for animal research.

Establishment of OM model and drug administration

Rats were randomly assigned into five groups (n=8 per group): normal control (NC), OM model (OM), and OM rats treated with low, medium, or high doses of SCYYD (OM+L, OM+M, OM+H). OM was induced in anesthetized rats (sodium pentobarbital, 50 mg/kg, i.p.) by placing a 9 mm² filter paper soaked in saturated sodium hydroxide in the labial fornix for 15 s, followed by intraperitoneal injection of methotrexate (25 mg/kg). SCYYD was administered intragastrically at doses of 7.3, 14.6, and 29.2 g/kg once daily for 8 days. NC and OM groups received equivalent volumes of saline. Body weights were monitored, and oral mucosal tissues were collected at the end of the experiment.

Assessment of oral mucosal healing

Oral mucosal recovery was evaluated using a standardized scoring system for OM, as detailed in **Table 1.**

Table 1. The scoring system of mucosal healing

Grade	Description	Mucosal Healing Score
Grade 0	No ulcer, normal oral mucosa	100
Grade I	Ulcer with no obvious pseudomembrane on the surface	80
Grade II	Ulcer with a thin yellow pseudomembrane on the surface	60
Grade III	The pseudomembrane on the surface of ulcer is thick, and there is inflammatory edema around it	40
Grade IV	The pseudomembrane on the surface of ulcer is very thick, and there is obvious inflammatory edema around it	20

Histopathological assessment

To examine structural changes in the oral mucosa, tissue samples from the labial fornix of the lower incisors were fixed in 10% formalin, dehydrated through a series of ethanol and xylene solutions, and embedded in paraffin. Sections of 5 μm thickness were prepared and stained with hematoxylin and eosin (H&E). The stained sections were then digitally scanned and analyzed using a NanoZoomer S60 Digital Slide Scanner (Hamamatsu, Japan) to evaluate tissue integrity, cellular organization, and pathological alterations.

RNA isolation and quantitative PCR (qPCR)

Total RNA was extracted from the oral mucosa using the Total RNA Rapid Extraction Kit (Beijing Biotek Biotechnology Co., Ltd., Beijing, China) following the manufacturer's instructions. RNA concentration and purity were determined using a Nanodrop One spectrophotometer (Thermo Scientific, USA). First-strand cDNA synthesis was carried out using the HiFiScript Quick gDNA Removal cDNA Kit (CoWin Biosciences, Jiangsu, China). Quantitative real-time PCR was performed with SYBR Green PCR Master Mix (CoWin Biosciences, Jiangsu, China) on a Roche 480 system (Roche, USA). Specific primers **(Table 2)** were synthesized by Sangon Biotech (Shanghai) Co., Ltd., with β-actin serving as the internal control. The PCR program included initial denaturation at 95°C for 10 min, followed by 45 cycles of 95°C for 10 s, 60°C for 30 s, and 72°C for 32 s. A melting curve analysis was conducted between 65°C and 97°C. Relative expression levels were calculated using the 2^−ΔΔCt method.

Table 2. Primer sequences for qPCR

Gene	Description	Sequence(5'-3')
Rat TNF	Forward Reverse	ATGGGCTCCCTCTCATCAGTTCC CCTCCGCTTGGTGGTTTGCTAC
Rat IL-1β	Forward Reverse	TTCAGGAAGGCAGTGTCACTCATTG TCATCATCCCACGAGTCACAGAGG
Rat IL-6	Forward Reverse	ACTTCCAGCCAGTTGCCTTCTTG TGGTCTGTTGTGGGTGGTATCCTC
Rat SRC	Forward Reverse	TCCCACATCCAAGCCTCAGACC CATCCACACCTCTCCGAAGCAAC
Rat HSP90AA1	Forward Reverse	AGCATAATGATGACGAGCAGTACGC CATTGGTTCACCTGTGTCTGTCCTC

Rat STAT3	Forward Reverse	AAAGGACATCAGTGGCAAGA CGGCAGGTCAATGGTATT
Rat MAPK3	Forward Reverse	GGACCTCATGGAGACGGACCTG CGGAGGATCTGGTAGAGGAAGTAGC
Rat ESR1	Forward Reverse	TCCTCCTCATCCTTTCCCATATCCG GCATCTCCAGCAGCAGGTCATAG
Rat HIF1α	Forward Reverse	CCGCCACCACCACTGATGAATC GTGAGTACCACTGTATGCTGATGCC
Rat TLR4	Forward Reverse	GGTGGTCAGTGTGCTTGTGGTAG CTCGTTTCTCACCCAGTCCTCATTC
Rat mTOR	Forward Reverse	AGATACGCCGTCATTCCT GCTCAAACACCTCCACCT
Rat MMP9	Forward Reverse	CACCGCCAACTATGACCAGGATAAG CTGCTTGCCCAGGAAGACGAAG
Rat PIK3CA	Forward Reverse	TGGCTATAAACGGGAACG TGCCGAATTGCTAGGTAC
Rat β-Actin	Forward Reverse	CGTGCGTGACATTAAAGAG CTGGAAGGTGGACAGTGAG

Statistical analysis

Data were expressed as mean ± standard error of the mean (SEM). Statistical analyses were performed using SPSS version 16.0 and GraphPad Prism 5. Differences between groups were assessed using Student's t-test or one-way ANOVA, and a p-value <0.05 was considered statistically significant.

Identification of bioactive compounds in SCYYD

A total of 555 chemical constituents of SCYYD were retrieved from the TCMSP database, comprising 51 from *Lithospermum erythrorhizon*, 60 from *Prunellae Spica*, 164 from *Menthae Herba*, and 280 from *Licorice*. Screening based on oral bioavailability (OB ≥ 30%) and drug-likeness (DL ≥ 0.18) identified 12 compounds (23.5%) from *Lithospermum erythrorhizon*, 11 compounds (18.3%) from *Prunellae Spica*, 10 compounds (6.1%) from *Menthae Herba*, and 92 compounds (32.9%) from *Licorice* that met the criteria **(Table 3).** After removing duplicates, a total of 119 compounds were considered as potential bioactive ingredients for further analysis.

Table 3. Number of ingredients in SCYYD with OB ≥30 and DL ≥0.18

Herbs	Total Ingredients	OB≥30	DL≥0.18	OB≥30 and DL≥0.18
Lithospermum Erythrorhizon	51	22(43.1)	35(68.6)	12(23.5)
Prunellae Spica	60	21(35.0)	39(65.0)	11(18.3)
Menthae Herba	164	94(57.3)	33(20.1)	10(6.1)
Licorice	280	143(51.1)	204(72.9)	92(32.9)

Acquisition of SCYYD ingredient targets relevant to OM

The chemical structures and SMILES notations of SCYYD compounds were retrieved from the PubChem database (https://pubchem.ncbi.nlm.nih.gov/). Potential molecular targets for these compounds were predicted using the SuperPred database. Following the removal of duplicates, 443 unique targets were retained for subsequent analyses. Additionally, 2,152 genes associated with oral mucositis were collected from GeneCards, OMIM, and DisGeNET databases. By identifying the overlap between SCYYD-related targets and OM-associated genes, 186 common targets were obtained, which are detailed in **Figure 2**.

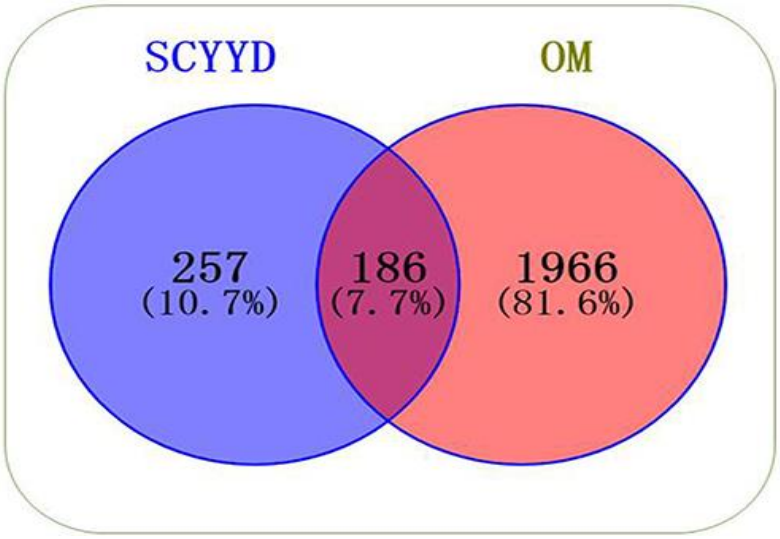

Figure 2. Venn diagram for the intersection of potential targets of SCYYD and OM-related genes.

Construction and analysis of the ingredient-target-disease network

To explore the relationships among the four herbs in SCYYD, their bioactive compounds, and potential targets associated with OM, an ingredient-target-disease network was established using Cytoscape 3.8.2. The resulting network included 299 nodes and 5,656 edges **(Figure 3)**, indicating that SCYYD likely acts through multiple compounds and targets. Based on degree values, the top ten key active compounds were identified as sitosterol, naringenin, kaempferol, quercetin, luteolin, glabridin, spinasterol, mairin, phaseolinisoflavan, and stigmasterol **(Table 4).** Notably, the top five compounds were present in more than one herb: sitosterol appeared in Lithospermum Erythrorhizon, Menthae Herba, and Licorice; naringenin in Menthae Herba and Licorice; kaempferol and quercetin in Prunellae Spica and Licorice; and luteolin in Prunellae Spica and Menthae Herba.

Table 4. The top 10 key active ingredients of SCYYD in the treatment of OM

Mol ID	Molecule Name	Degree	OB(%)	DL	Source
MOL000359	Sitosterol	144	36.91	0.75	Lithospermum Erythrorhizon, Menthae Herba, and Licorice
MOL004328	Naringenin	104	59.29	0.21	Menthae Herba and Licorice
MOL000422	Kaempferol	92	41.88	0.24	Prunellae Spica and Licorice
MOL000098	Quercetin	86	46.43	0.28	Prunellae Spica and Licorice
MOL000006	Luteolin	84	36.16	0.25	Prunellae Spica and Menthae Herba
MOL004908	Glabridin	66	53.25	0.47	Licorice
MOL004355	Spinasterol	66	42.98	0.76	Prunellae Spica
MOL000211	Mairin	64	55.38	0.78	Licorice
MOL004833	Phaseolinisoflavan	63	32.01	0.45	Licorice
MOL000449	Stigmasterol	63	43.83	0.76	Prunellae Spica

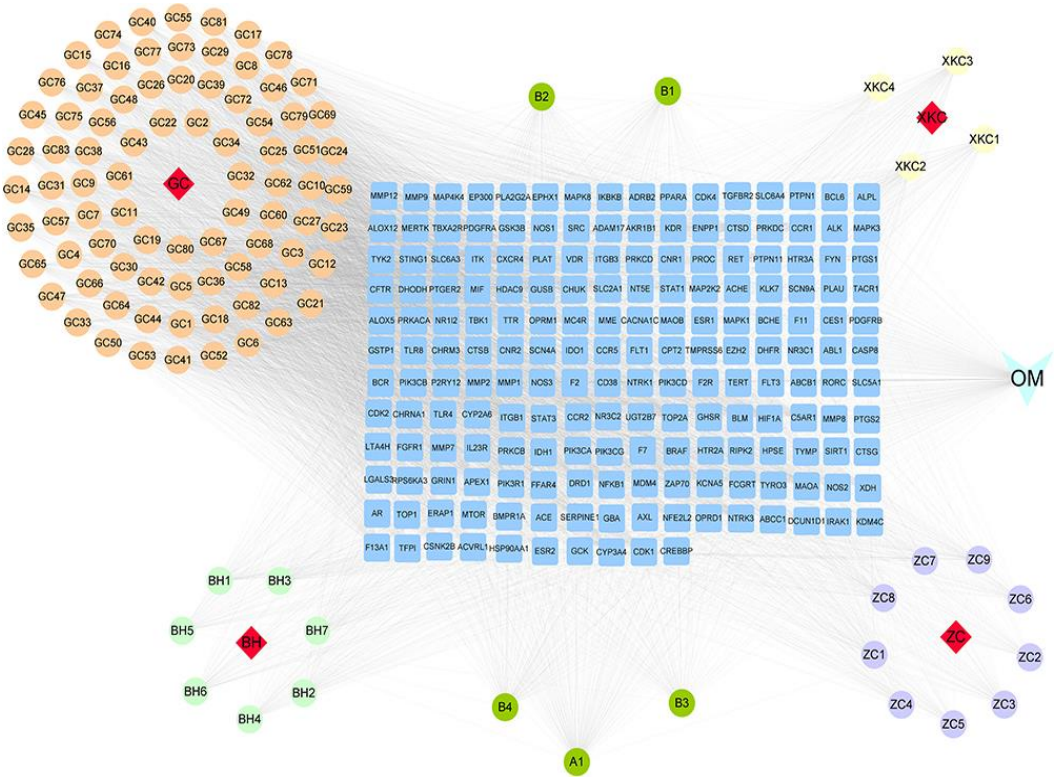

Figure 3. The ingredient-target-disease network of SCYYD on OM. There were 4 kinds of herbs, 108 active ingredients, 186 target genes. The diamond represents herbs in SCYYD, the circle represents the active ingredients of SCYYD, the rectangle represents the target genes, and the V shape represents for OM.

Figure construction of the PPI network and screening of key targets

To investigate potential protein interactions, a PPI network was established using the STRING database, consisting of 183 nodes connected by 1,892 edges, and visualized with Cytoscape 3.8.2 **(Figure 4a)**. Using the Cytohubba plugin, the ten proteins with the highest connectivity were identified as central nodes, including SRC, HSP90AA1, STAT3, MAPK3, ESR1, HIF1α, TLR4, mTOR, MMP9, and PIK3CA **(Figures 4b–4c).**

MCODE analysis further divided the network into eight clusters of highly interconnected targets **(Figure 5)**. Cluster 1, with the highest clustering score, comprised 31 nodes and 245 interactions. Biological process (BP) enrichment revealed 64 significant terms for cluster 1, 32 for cluster 2, 33 for cluster 3, and fewer in other clusters ($P < 0.05$, FDR < 0.05).

Functional analysis indicated that cluster 1 was primarily associated with transcriptional regulation and inflammatory processes, including negative regulation of gene expression, positive regulation of RNA polymerase II–mediated transcription, angiogenesis, inflammatory response, and inhibition of endothelial apoptosis. Cluster 2 was enriched in stress responses and apoptosis-related processes, such as responses to reactive oxygen species, cadmium ions, UV exposure, and serine phosphorylation. Cluster 3 focused on signaling and migration pathways, including tyrosine phosphorylation, transmembrane receptor tyrosine kinase signaling, protein phosphorylation, cell migration, and positive regulation of kinase activity.

These results suggest that SCYYD may exert therapeutic effects on oral mucositis through multiple interconnected targets and biological pathways, involving transcriptional regulation, inflammation, oxidative stress response, and cell signaling.

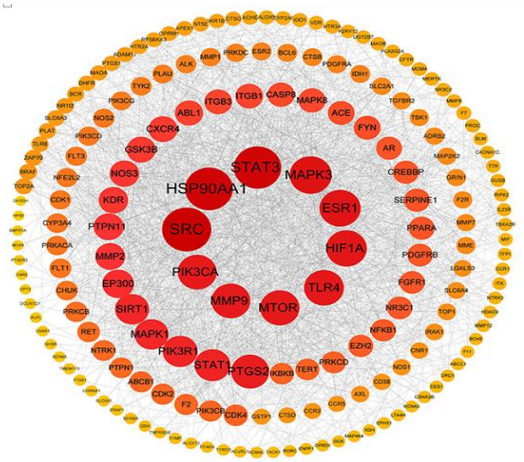

a)

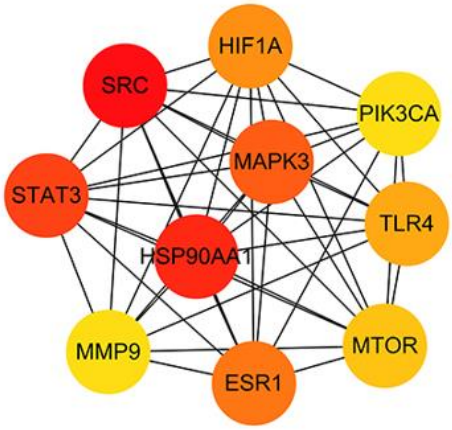

b)

Ranking Method(Degree)	
Rank	Node
1	SRC
2	HSP90AA1
3	STAT3
4	MAPK3
5	ESR1
6	HIF1A
7	TLR4
8	MTOR
9	MMP9
9	PIK3CA

c)

Figure 4. PPI network of SCYYD against OM. (a) The PPI network with 183 nodes and 1892 edges is constructed by Cytoscape. Node size is proportional to the number of degree. The node degree is gradually larger when the color is from yellow to red. (b)The top 10 core genes collected from (a). (c) The core targets list for SCYYD on OM by Degree method

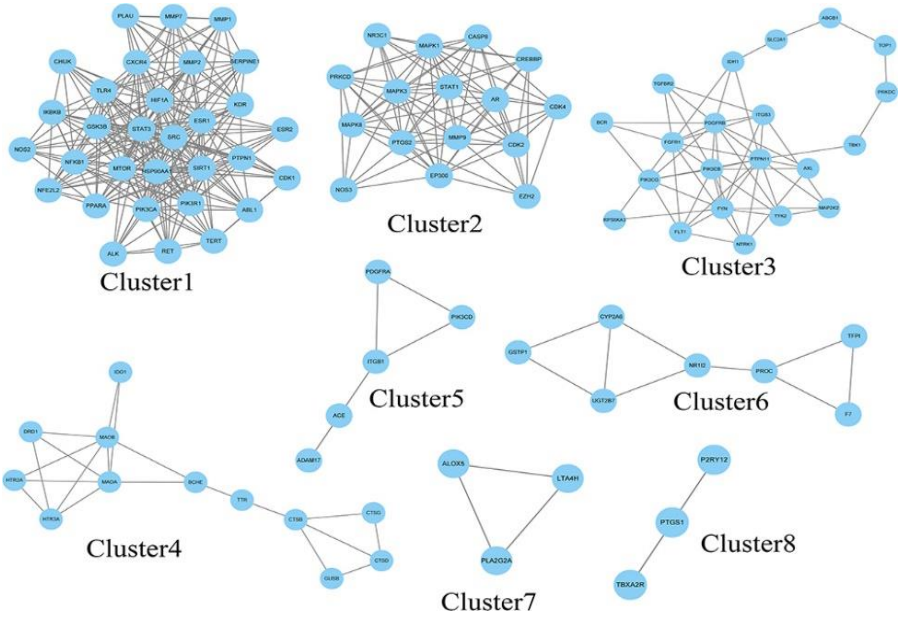

Figure 5. The gene clusters of SCYYD against OM. The cluster from 1 to 8 is based on their cluster score.

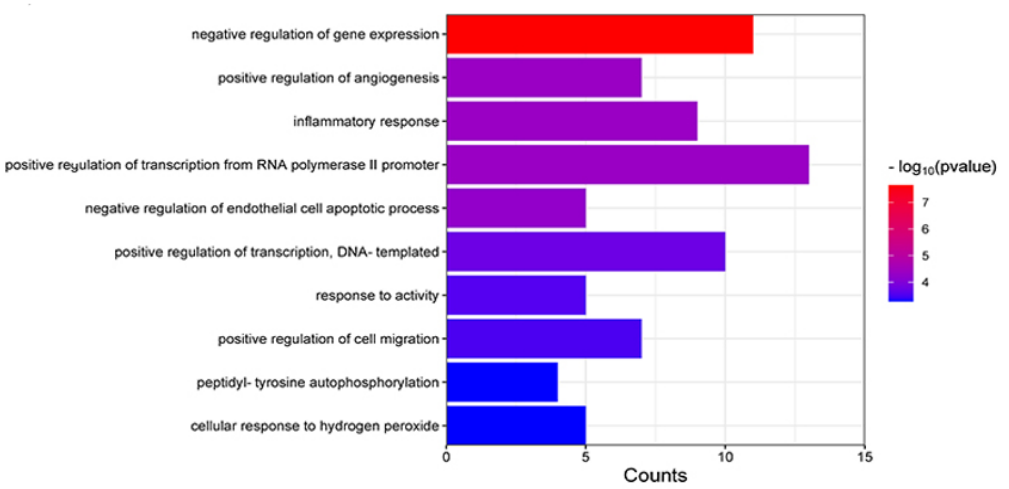

a)

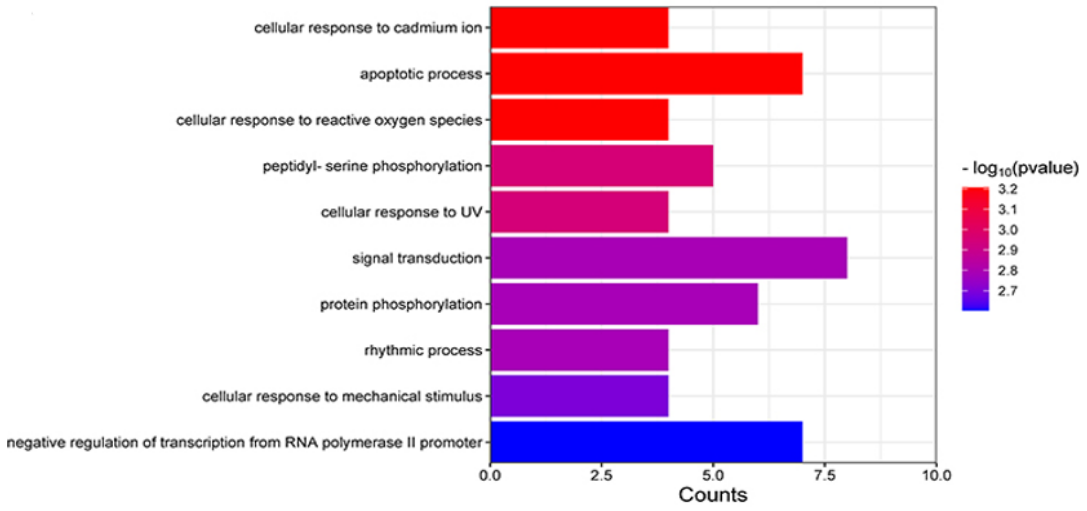

b)

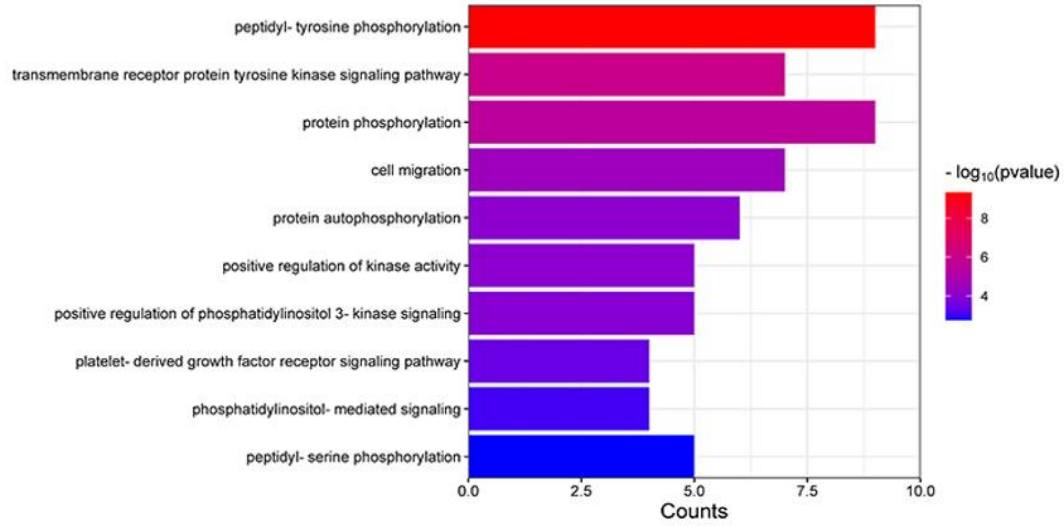

c)

Figure 6. The BP for gene clusters of SCYYD against OM. (a) The top 10 BP terms of Cluster 1. (b) The top 10 BP terms of Cluster 2. (c) The top 10 BP terms of Cluster

GO and KEGG enrichment and target-pathway analysis

To understand the potential mechanisms of SCYYD in treating OM, we conducted Gene Ontology (GO) enrichment analysis on 186 predicted target genes. A total of 404 significant GO terms were identified ($P < 0.05$, FDR < 0.05), including 283 related to biological processes (BP), 53 to cellular components (CC), and 68 to molecular functions (MF). **Figure 7** displays the top 10 terms from each category, ranked by q-value.

In the BP category, the most prominent terms were cytokine-mediated signaling pathway (GO:0019221), inflammatory response (GO:0006954), protein phosphorylation (GO:0006468), peptidyl-tyrosine phosphorylation (GO:0018108), and platelet activation (GO:0030168). For CC, the targets were mainly associated with structures at the cell surface and plasma membrane, including plasma membrane (GO:0005886), receptor complex (GO:0043235), cell surface (GO:0009986), integral component of plasma membrane (GO:0005887), and membrane raft (GO:0045121). MF analysis highlighted activities related to kinase functions and ATP binding, such as protein serine/threonine/tyrosine kinase activity (GO:0004712), transmembrane receptor protein tyrosine kinase activity (GO:0004714), protein tyrosine kinase activity (GO:0004713), ATP binding (GO:0005524), and protein serine/threonine kinase activity (GO:0004674).

Overall, these results indicate that SCYYD may influence OM through pathways involving inflammatory signaling, phosphorylation cascades, and interactions with membrane-associated receptor complexes.

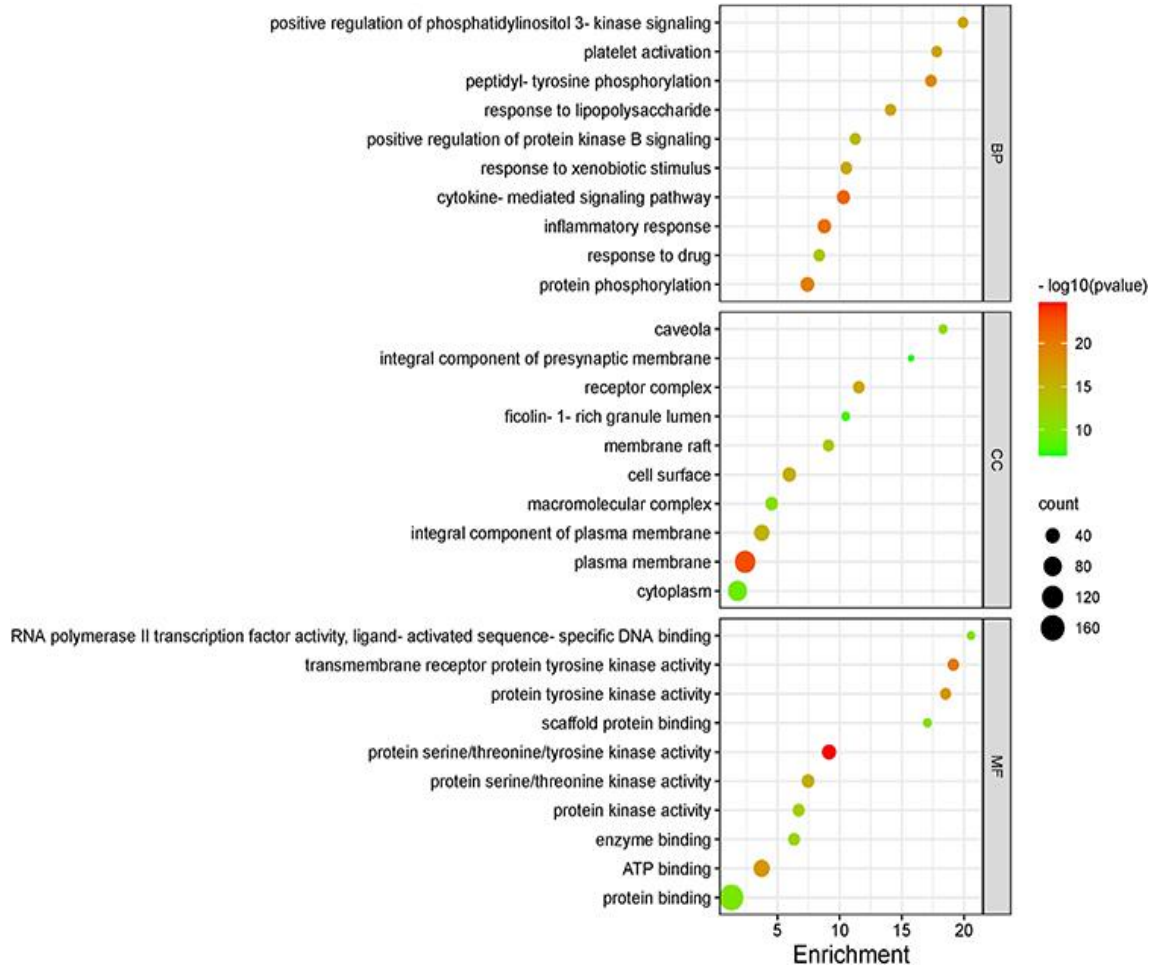

Figure 7. The top 10 of GO enrichment analysis for target genes of SCYYD against OM.

To investigate how SCYYD may act against OM at the pathway level, we performed KEGG enrichment analysis. This revealed 160 pathways with significant enrichment ($P < 0.05$, FDR < 0.05). The 20 pathways most closely linked to OM are illustrated in **Figure 8**, highlighting, among others, the HIF-1 and Ras signaling pathways.

We then constructed a network connecting these pathways with their associated genes to clarify SCYYD's molecular mechanisms in OM **(Figure 9).** Pathways with the highest number of mapped genes included "Pathways in cancer" (53 genes), Kaposi's sarcoma-associated herpesvirus infection (27), human cytomegalovirus infection (27), hepatitis B (26), chemical carcinogenesis–receptor activation (26), and the Ras

signaling pathway (26). Within these pathways, several key genes were consistently enriched, including PIK3CD, PIK3CB, PIK3CA, PIK3R1, MAPK1, MAPK3, MAP2K2, NFKB1, STAT3, IKBKB, and mTOR.

These results indicate that SCYYD likely exerts its therapeutic effects on OM through the modulation of multiple signaling cascades and critical regulatory genes, suggesting a multi-target mechanism underlying its pharmacological action.

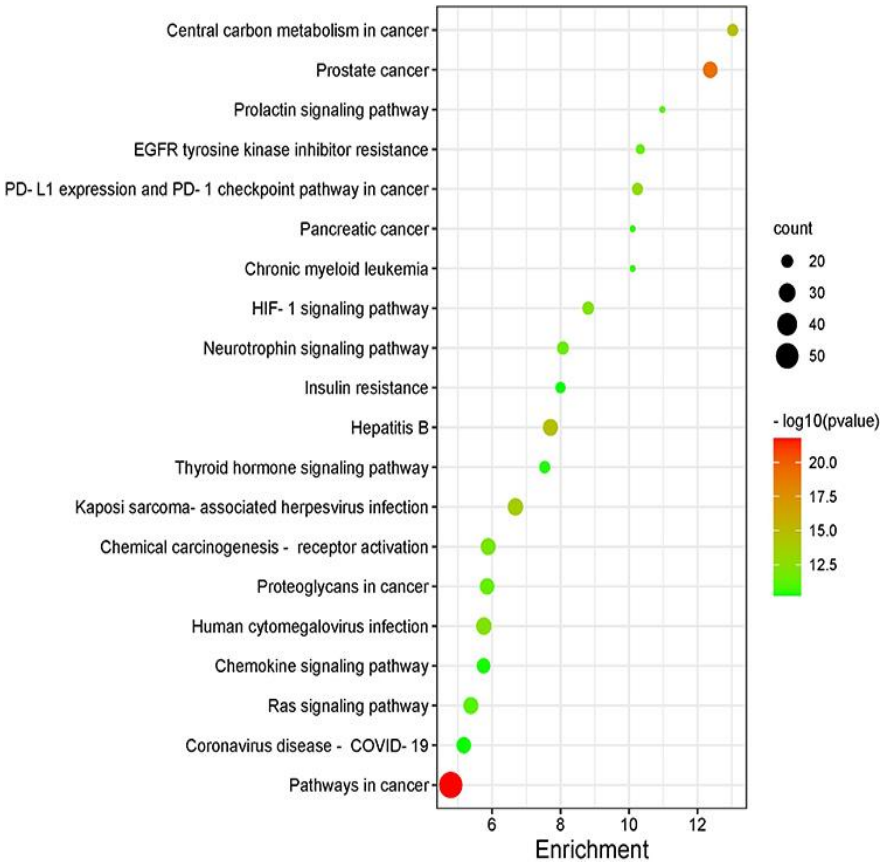

Figure 8. The top 20 signaling pathways from KEGG enrichment analysis of target genes of SCYYD against OM.

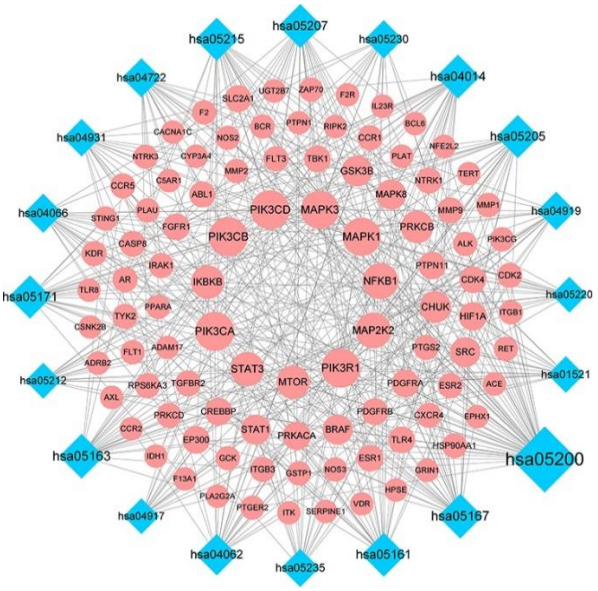

Figure 9. The target-pathway network of SCYYD against OM. The blue nodes stand for pathways and the red nodes stand for target genes. The node size is proportional to the number of degree.

Binding ability between the active ingredients and key targets by molecular docking

Molecular docking was performed using CB-Dock2 to evaluate the binding interactions between the five most prominent active compounds identified from the ingredient-target-disease network (sitosterol, naringenin, kaempferol, quercetin, and luteolin) and the core proteins (SRC, HSP90AA1, STAT3, ESR1, and HIF1α). The docking results were quantified using vina scores, where higher absolute values indicate stronger binding affinity and stability between a compound and its target. Specifically, an absolute vina score above 4.25 suggests measurable binding, above 5.0 indicates good binding affinity, and above 7.0 reflects strong binding interaction [15].

As summarized in **Table 5,** most compound-target pairs exhibited absolute vina scores exceeding 7.0, demonstrating strong binding of these five active ingredients to SRC, HSP90AA1, STAT3, and HIF1α. The interaction with ESR1 showed scores between 5.0 and 7.0, reflecting moderate to good binding. Representative 3D docking conformations for each compound-target pair are displayed in **Figure 10.**

Table 5. Binding energy between key ingredients and target proteins

Key Ingredients	Vina Score				
	SRC(1A07)	HSP90AA1(3Q6M)	STAT3(6QHD)	ESR1(6KN5)	HIF1α(4H6J)
Sitosterol	−7.6	−8.2	−8.1	−7.2	−7.6
Naringenin	−7.8	−8.6	−8.5	−6.1	−7.6
Kaempferol	−8.0	−9.0	−8.8	−6.2	−8.0
Quercetin	−8.5	−9.0	−9.2	−6.3	−8.0
Luteolin	−8.1	−8.3	−9.2	−6.3	−7.5

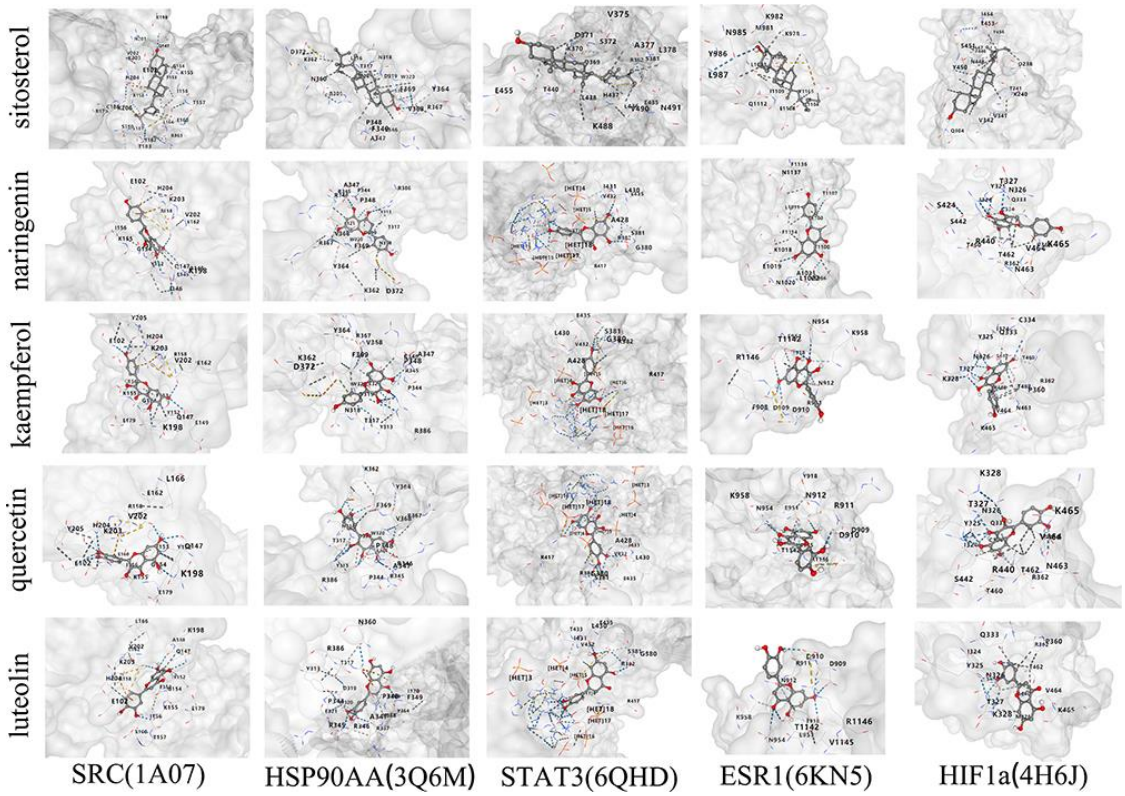

Figure 10. The 3D map of each docking diagram.

SCYYD improved oral mucositis symptoms

The therapeutic effect of SCYYD on oral mucositis (OM) was assessed in vivo using a rat model. OM was induced in rats, which were then treated with SCYYD via oral administration. Body weight and mucosal healing scores were recorded, followed by histological analysis of oral mucosa using H&E staining. As illustrated in **Figure 11a**,

rats in the OM group exhibited significantly reduced body weight compared with the normal control (NC) group ($P < 0.01$). Treatment with medium- and high-dose SCYYD (OM+M and OM+H) significantly improved body weight relative to the untreated OM group ($P < 0.01$), whereas the low-dose SCYYD group (OM+L) showed no significant difference compared with the OM group ($P > 0.05$).

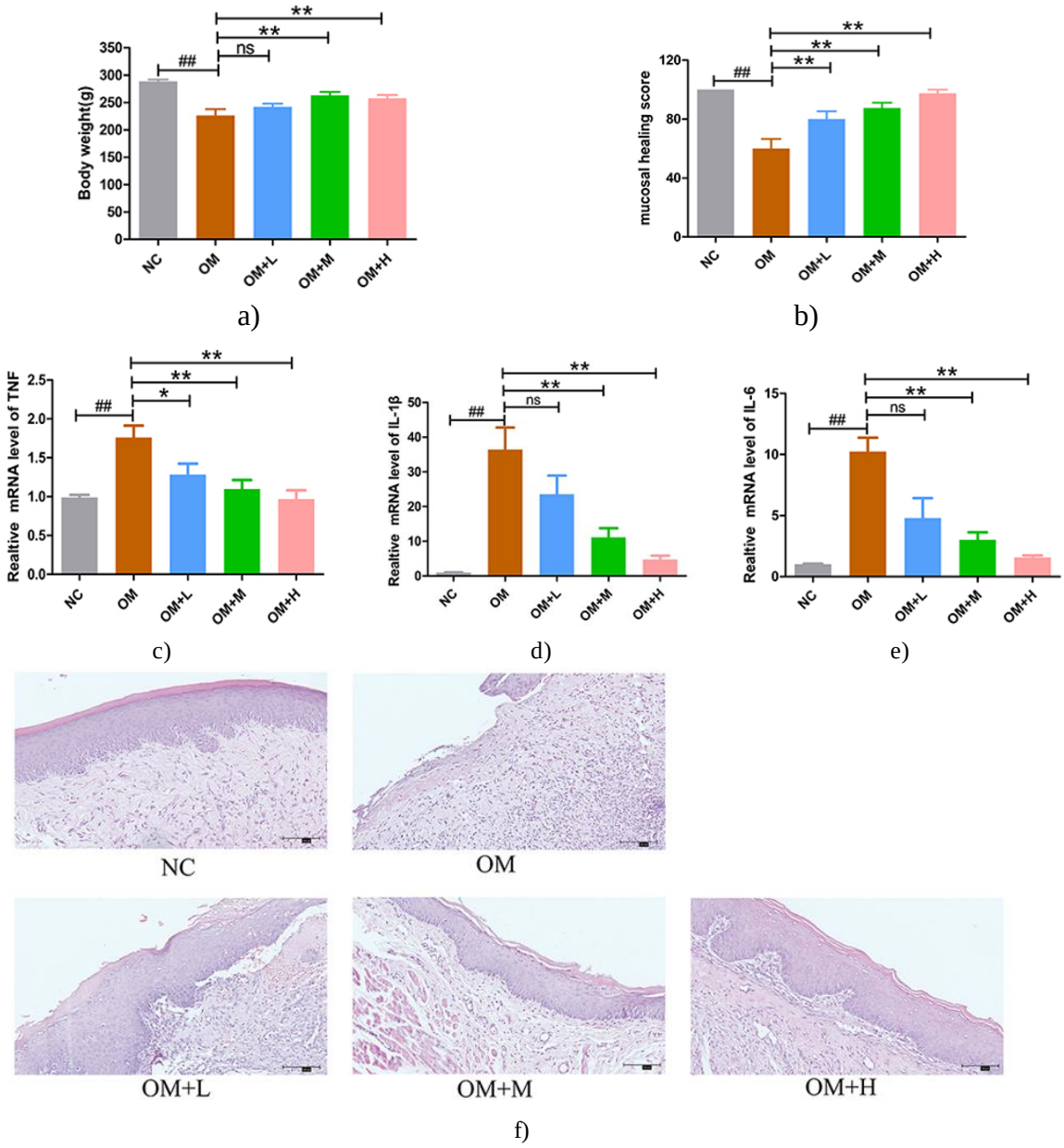

Figure 11. SCYYD exerts wound healing effect in OM rats. (a)The body weight in each group. (b) The mucosal healing score in each group. (c-e) The mRNA expressions of TNF, IL-1β and IL-6 were examined by qPCR. β-actin was used as an internal control. (f) The histopathology of oral mucosa in each group. Bar=100μm. Data are expressed as mean±SEM. ##$P < 0.01$ versus NC group, *$P < 0.05$ versus OM group, **$P < 0.01$ versus OM group.

SCYYD Promoted healing in OM rats

The therapeutic effect of SCYYD on oral mucositis (OM) was evaluated in vivo. Throughout the experiment, the oral mucosa of rats in the OM group exhibited thick pseudomembranes over ulcerated areas, accompanied by marked inflammatory edema. Administration of SCYYD at various doses significantly accelerated mucosal recovery. As shown in **Figure 11b**, the mucosal healing scores of OM rats were markedly lower than those of the normal control (NC) group ($P < 0.01$). Treatment with low, medium, and high doses of SCYYD significantly

improved healing scores compared with the OM group ($P < 0.01$), demonstrating the efficacy of SCYYD in promoting mucosal repair.

SCYYD suppressed inflammatory responses in OM

To assess the anti-inflammatory effects of SCYYD, mRNA levels of key pro-inflammatory cytokines in oral mucosa were analyzed by qPCR. The OM group displayed elevated expression of TNF, IL-1β, and IL-6 compared with NC rats ($P < 0.01$); **(Figures 11c–11e**). Following SCYYD treatment, TNF expression was significantly reduced in all treatment groups (OM+L, OM+M, OM+H; $P < 0.05$ or $P < 0.01$), whereas IL-1β and IL-6 expression decreased significantly in the medium- and high-dose groups (OM+M and OM+H; $P < 0.01$). These findings indicate that SCYYD effectively mitigates inflammatory signaling in OM.

Histopathological improvement of OM by SCYYD

Histological analysis further confirmed the therapeutic effect of SCYYD. The NC group exhibited intact epithelial layers with no inflammatory cell infiltration, whereas the OM group showed severe ulceration, disrupted epithelium, and abundant inflammatory infiltration. Reepithelization was initiated in the low-dose SCYYD group (OM+L), but recovery remained incomplete with persistent inflammatory cells. The medium-dose group (OM+M) displayed more advanced epithelial regeneration with reduced inflammation. The high-dose group (OM+H) showed almost complete epithelial recovery and minimal inflammatory infiltration, indicating dose-dependent efficacy **(Figure 11f).**

Validation of key targets of SCYYD in OM

To corroborate the key targets identified through network pharmacology, the mRNA expressions of SRC, HSP90AA1, STAT3, MAPK3, ESR1, HIF1α, TLR4, mTOR, MMP9, and PIK3CA were examined by qPCR **(Figure 12).** In OM rats, SRC, HSP90AA1, STAT3, HIF1α, TLR4, mTOR, and MMP9 levels were significantly elevated compared with NC ($P < 0.01$ or $P < 0.05$). Treatment with SCYYD at all doses reduced SRC, HSP90AA1, STAT3, HIF1α, TLR4, and mTOR expression ($P < 0.05$ or $P < 0.01$), while MMP9 expression was significantly decreased in the medium- and high-dose groups. Conversely, ESR1 and PIK3CA expression was lower in OM rats relative to NC ($P < 0.01$); medium- and high-dose SCYYD increased ESR1 expression significantly ($P < 0.05$ or $P < 0.01$), whereas PIK3CA levels remained unchanged following treatment ($P > 0.05$).

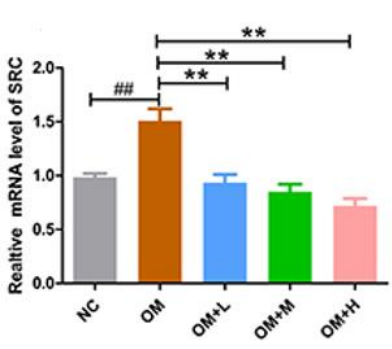

a)

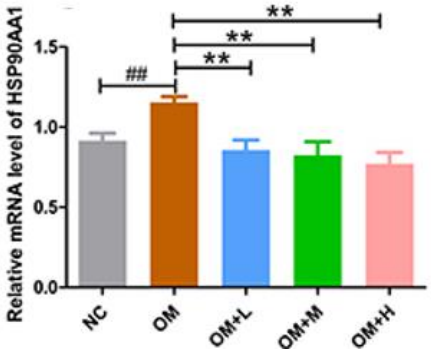

b)

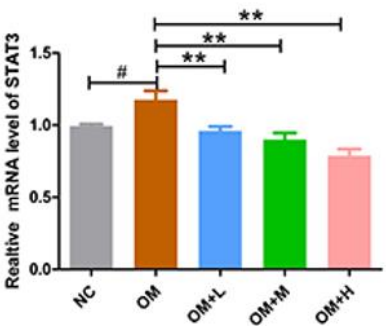

c)

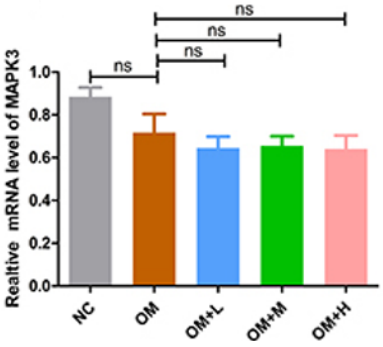

d)

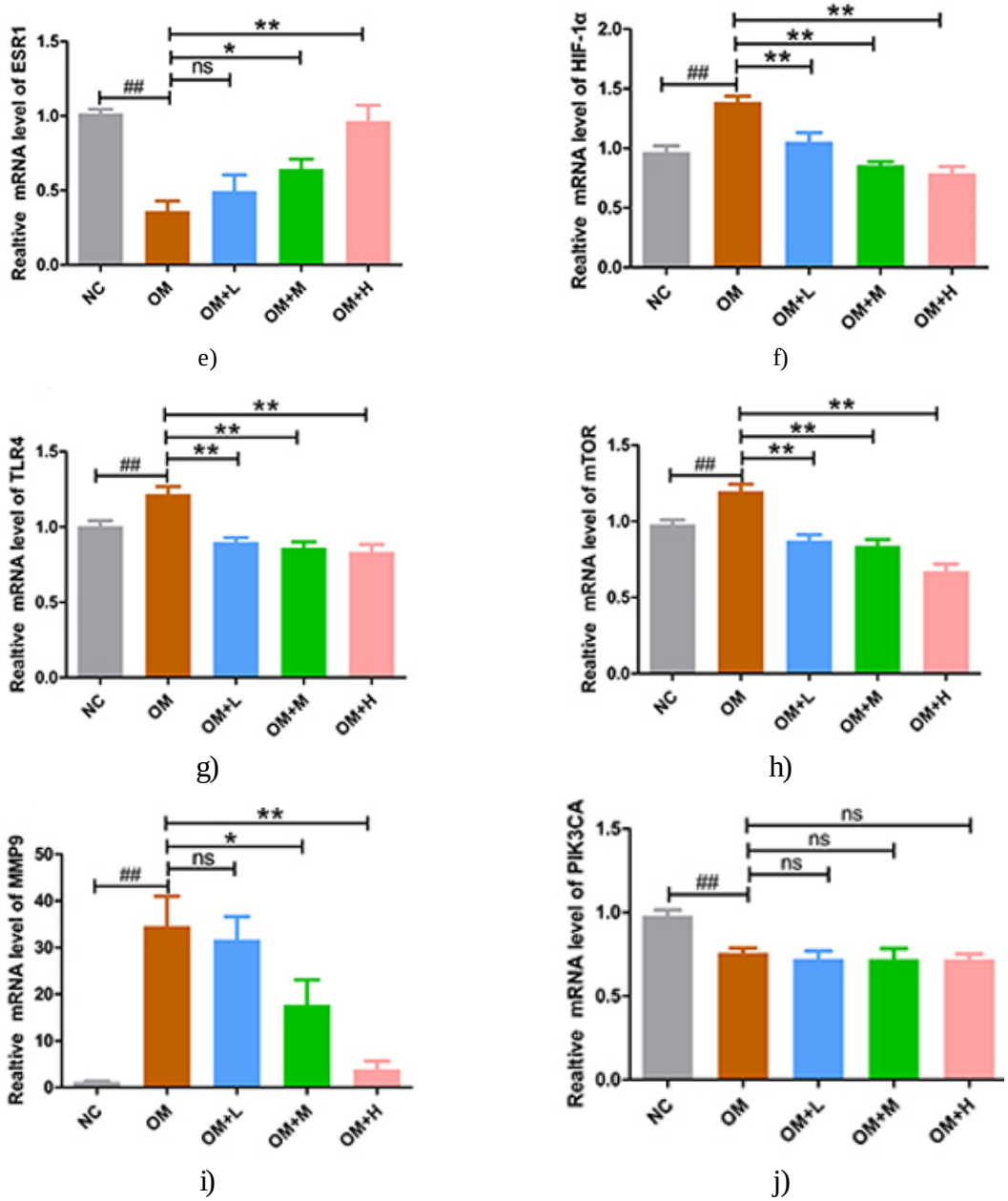

Figure 12. The mRNA expression levels of the main key targets were analyzed by qPCR. Panels (A–J) show the expression of SRC, HSP90AA1, STAT3, MAPK3, ESR1, HIF1α, TLR4, mTOR, MMP9, and PIK3CA, with β-actin as the internal control. Data are presented as mean ± SEM. #P < 0.05 vs. NC group, ##P < 0.01 vs. NC group, *P < 0.05 vs. OM group, **P < 0.01 vs. OM group.

Results and Discussion

Oral mucositis (OM) is a recurrent condition with a complex etiology involving multiple signaling pathways. It is primarily characterized by painful and inflamed lesions that can occur anywhere in the oral cavity. Consequently, herbs with heat-clearing and detoxifying properties are increasingly used in OM treatment due to their anti-inflammatory and antioxidant effects [9, 16]. SCYYD exhibits these properties and has been shown to be effective against chemotherapy-induced OM by reducing inflammatory mediators [12].

In this study, a rat model of OM was established through combined mucosal injury using sodium hydroxide and methotrexate chemotherapy, which produced persistent ulceration suitable for evaluating therapeutic effects [17]. Administration of SCYYD at different doses improved erythema, erosions, and ulcerations while reducing inflammatory factors, demonstrating its anti-inflammatory and mucosal healing effects. However, due to its multi-component and multi-target characteristics, the molecular mechanisms of SCYYD in OM are not fully understood.

Network pharmacology, integrating systems biology and bioinformatics, provides a comprehensive method to investigate such complex mechanisms and has been widely applied to elucidate multi-target and multi-pathway effects of traditional Chinese medicines [18–20]. In the present study, we combined network pharmacology with experimental validation to explore the effects and mechanisms of SCYYD against OM.

Pharmacokinetic properties are crucial for ensuring that bioactive compounds reach target tissues and exert therapeutic effects [21]. A total of 119 bioactive compounds were identified using OB ≥30% and DL ≥0.18 as criteria. The major active ingredients included sitosterol, naringenin, kaempferol, quercetin, and luteolin. Sitosterol, a phytosterol, can reduce chronic inflammation by downregulating IL-6 and TNF-α [22]. Naringenin, a citrus flavonoid, has anti-inflammatory, antioxidant, anticancer, and antiatherogenic activities and acts as an immunomodulator [23, 24]. Kaempferol exhibits diverse pharmacological effects including anti-inflammatory, antioxidant, anticancer, antimicrobial, cardioprotective, and neuroprotective actions, partly through inhibition of STAT3-mediated inflammatory signaling [25–28]. Quercetin also possesses anti-inflammatory, antioxidant, and anticancer activities, alleviating inflammation via NF-κB inhibition in chemotherapy- or radiation-induced OM models [29, 30]. Luteolin similarly exerts anti-inflammatory effects by regulating transcription factors such as STAT3, NF-κB, and AP-1 [31, 32]. Collectively, these compounds support the predicted anti-inflammatory actions of SCYYD in OM.

Network pharmacology identified 186 potential target genes. GO enrichment analysis revealed that most targets were associated with inflammatory responses, a key pathogenic factor of OM. KEGG pathway enrichment indicated that these targets were predominantly involved in immune and inflammatory signaling, tumorigenesis, and viral infection pathways. For example, the HIF-1 signaling pathway can be activated by oxidative stress, leading to expression of genes related to inflammation, cytokines, growth factors, and chemokines [33]. Module analysis further highlighted mechanisms related to inflammatory responses and cellular responses to reactive oxygen species, suggesting that SCYYD exerts anti-inflammatory and antioxidant effects.

PPI network analysis identified core targets including SRC, HSP90AA1, STAT3, MAPK3, ESR1, HIF1α, TLR4, mTOR, MMP9, and PIK3CA. SRC, a cytoplasmic tyrosine kinase, regulates neutrophil functions such as ROS production, NET formation, integrin activation, and migration to inflamed sites [34]. HSP90AA1 encodes Hsp90α, a conserved chaperone protein involved in inflammation, and Hsp90 inhibitors have anti-inflammatory effects [35, 36]. STAT3 plays a crucial role in oral mucosal homeostasis by controlling inflammatory cytokine production, and its polymorphisms may predispose to OM [37]. MAPK3 regulates autoimmune responses [38], while ESR1 encodes ERα, modulating immune pathways and suppressing NF-κB signaling [39]. HIF1α is upregulated by metal ions, nitric oxide, and cytokines such as IL-1β and TNF-α, and is significantly increased in irradiated oral mucosa [40]. TLR4 recognizes LPS or DAMPs, activating innate and adaptive immunity and promoting pro-inflammatory cytokine production [41, 42]. mTOR is an atypical serine/threonine kinase involved in PIKK signaling, and its downregulation can counteract inflammation [43, 44]. MMPs, especially MMP9, contribute to OM by damaging submucosal tissue and disrupting epithelial integrity [45]. PIK3CA encodes the p110α catalytic subunit of PI3K, increasing tumor susceptibility in oral carcinogenesis models [46].

Consistent with these reports, our animal experiments showed that SCYYD treatment reduced expression of SRC, HSP90AA1, STAT3, HIF1α, TLR4, mTOR, and MMP9, while ESR1 expression was increased. These findings confirm the multi-target action of SCYYD and demonstrate the critical role of these genes in OM, providing mechanistic insight into its therapeutic effects.

Subsequently, molecular docking was employed to confirm the specific interactions between the key active compounds and core protein targets. The docking results indicated that the main ingredients in SCYYD exhibited strong binding affinities with the identified targets, suggesting that these compounds may mediate the therapeutic effects of SCYYD on OM through modulation of these proteins and their associated signaling pathways. This provides a foundation for further investigation into natural compounds for OM treatment.

Nevertheless, several limitations exist in the present study. First, the public databases used for screening SCYYD's bioactive compounds and OM-related targets are not exhaustive, which may have resulted in the omission of other relevant compounds or genes. In addition, further experimental validation is required to confirm additional targets and signaling pathways through which SCYYD exerts its effects. Despite these limitations, this study provides preliminary insight into the mechanisms of SCYYD against OM and offers a basis for the development of novel anti-inflammatory therapies for OM.

Conclusion

In conclusion, by integrating network pharmacology, molecular docking, and in vivo experimentation, this study elucidated the potential mechanisms by which SCYYD treats OM. The findings suggest that SCYYD acts on multiple targets and engages various signaling pathways to produce therapeutic effects. While further research is needed to clarify the precise mechanisms, this study systematically identifies the probable targets and pathways of SCYYD, providing an experimental foundation for its clinical application in OM management.

Acknowledgments: This study was supported by Hangzhou Medical and Health Science and Technology Key Project (No. 0020190586); Zhejiang Famous Traditional Chinese Medicine Expert Inheritance Studio Construction Project Liu Yunxia Famous Traditional Chinese Medicine Expert Inheritance Studio (No. GZS2020030)

Conflict of Interest: None

Financial Support: None

Ethics Statement: This study is involving human data from public databases GeneCards, OMIM and DisGeNET. Due to GeneCards, OMIM and DisGeNET belong to public databases and users can download relevant data for free for research and publish relevant articles, the ethics committee of Hangzhou Third People's Hospital confirms that this study would have had the need for ethics approval waived.

References

1. Peterson DE, Boers-Doets CB, Bensadoun RJ, Herrstedt J; ESMO Guidelines Committee. Management of oral and gastrointestinal mucosal injury: ESMO Clinical Practice Guidelines for diagnosis, treatment, and follow-up. Ann Oncol. 2015;26 Suppl 5:v139-51. doi:10.1093/annonc/mdv202
2. Rubenstein EB, Peterson DE, Schubert M, Keefe D, McGuire D, Epstein J, et al. Clinical practice guidelines for the prevention and treatment of cancer therapy-induced oral and gastrointestinal mucositis. Cancer. 2004;100(9):2026-46. doi:10.1002/cncr.20163
3. Pulito C, Cristaudo A, Porta C, Zapperi S, Blandino G, Morrone A, et al. Oral mucositis: the hidden side of cancer therapy. J Exp Clin Cancer Res. 2020;39(1):210. doi:10.1186/s13046-020-01715-7
4. Jung YS, Park EY, Sohn HO. Oral health status and oral health-related quality of life according to presence or absence of mucositis in head and neck cancer patients. J Cancer Prev. 2019;24(1):43–7. doi:10.15430/JCP.2019.24.1.43
5. Park JW, Oh J, Ko SJ, Chang MS, Kim J. Effects of Onchung-eum, an Herbal Prescription, on 5-Fluorouracil-Induced Oral Mucositis. Integr Cancer Ther. 2018;17(4):1285-96. doi:10.1177/1534735418805560. Epub 2018 Oct 8
6. Wang G, Jia L. Herb medicine for relieving radiation induced oral mucositis: a systematic review and meta-analysis protocol. Medicine. 2019;98(50):18337. doi:10.1097/MD.0000000000018337
7. Sio TT, Le-Rademacher JG, Leenstra JL, Loprinzi CL, Rine G, Curtis A, et al. Effect of Doxepin Mouthwash or Diphenhydramine-Lidocaine-Antacid Mouthwash vs Placebo on Radiotherapy-Related Oral Mucositis Pain: the alliance A221304 randomized clinical trial. JAMA. 2019;321(15):1481-90. doi:10.1001/jama.2019.3504
8. Meyer-Hamme G, Beckmann K, Radtke J, Efferth T, Greten HJ, Rostock M, et al. A survey of chinese medicinal herbal treatment for chemotherapy-induced oral mucositis. Evid Based Complement Alternat Med. 2013;2013:284959. doi:10.1155/2013/284959
9. Lin Z, Chen J, Han S. The efficacy of heat-clearing (Qingre) and detoxifying (Jiedu) traditional Chinese medicine gargle for chemotherapy-induced oral mucositis: a systematic review and meta-analysis. Front Pharmacol. 2021;12:627628. doi:10.3389/fphar.2021.627628
10. Geng QS, Liu RJ, Shen ZB, Wei Q, Zheng YY, Jia LQ, et al. Transcriptome sequencing and metabolome analysis reveal the mechanism of Shuanghua Baihe Tablet in the treatment of oral mucositis. Chin J Nat Med. 2021;19(12):930-43. doi:10.1016/S1875-5364(22)60150-X

11. Sheng P, Xie J, Wu Y, Xia X, Li B, Wu M. A Network Pharmacology Approach for Uncovering the Mechanism of 'Kouchuangling' in Radiation-induced Oral Mucositis Treatment. Comb Chem High Throughput Screen. 2023;26(5):1042-57. doi:10.2174/1386207325666220617151600
12. Yunxia L, Yefeng X, Shuai L, et al. Clinical study on prevention and treatment of Sancao Yuyang Decoction on oral mucositis of patients with osteosarcoma after high-dose Methotrexate chemotherapy. China J Traditional Chine Med Pharm. 2019;34(10):4942–6.
13. Zhang R, Zhu X, Bai H, Ning K. Network Pharmacology Databases for Traditional Chinese Medicine: Review and Assessment. Front Pharmacol. 2019;10:123. doi:10.3389/fphar.2019.00123
14. Li S, Zhang B. Traditional Chinese medicine network pharmacology: theory, methodology and application. Chin J Nat Med. 2013;11(2):110–20. doi:10.1016/S1875-5364(13)60037-0
15. Hsin KY, Ghosh S, Kitano H. Combining machine learning systems and multiple docking simulation packages to improve docking prediction reliability for network pharmacology. PLoS One. 2013;8(12): 83922. doi:10.1371/journal.pone.0083922
16. Tanideh N, Namazi F, Andisheh Tadbir A, Ebrahimi H, Koohi-Hosseinabadi O. Comparative assessment of the therapeutic effects of the topical and systemic forms of Hypericum perforatum extract on induced oral mucositis in golden hamsters. Int J Oral Maxillofac Surg. 2014;43(10):1286-92. doi:10.1016/j.ijom.2014.05.013
17. Takeuchi I, Kawamata R, Makino K, Rat A. model of oral mucositis induced by cancer chemotherapy for quantitative experiments. Anticancer Res. 2020;40(5):2701–6. doi:10.21873/anticanres.14241
18. He S, Wang T, Shi C, et al. Network pharmacology-based approach to understand the effect and mechanism of Danshen against anemia. J Ethnopharmacol. 2022;282:114615. doi:10.1016/j.jep.2021.114615
19. Dong Y, Zhao Q, Wang Y. Network pharmacology-based investigation of potential targets of astragalus membranaceous-angelica sinensis compound acting on diabetic nephropathy. Sci Rep. 2021;11(1):19496. doi:10.1038/s41598-021-98925-6
20. Zhou W, Zhang H, Wang X, Kang J, Guo W, Zhou L, et al. Network pharmacology to unveil the mechanism of Moluodan in the treatment of chronic atrophic gastritis. Phytomedicine. 2022;95:153837. doi:10.1016/j.phymed.2021.153837
21. Obach RS, Baxter JG, Liston TE, Silber BM, Jones BC, MacIntyre F, et al. The prediction of human pharmacokinetic parameters from preclinical and in vitro metabolism data. J Pharmacol Exp Ther. 1997;283(1):46-58
22. Kurano M, Hasegawa K, Kunimi M, Hara M, Yatomi Y, Teramoto T, et al. Sitosterol prevents obesity-related chronic inflammation. Biochim Biophys Acta Mol Cell Biol Lipids. 2018;1863(2):191-8. doi:10.1016/j.bbalip.2017.12.004
23. Patel K, Singh GK, Patel DK. A Review on pharmacological and analytical aspects of naringenin. Chin J Integr Med. 2018;24(7):551–60. doi:10.1007/s11655-014-1960-x
24. Zeng W, Jin L, Zhang F, Zhang C, Liang W. Naringenin as a potential immunomodulator in therapeutics. Pharmacol Res. 2018;135:122-6. doi:10.1016/j.phrs.2018.08.002
25. Calderón-Montaño JM, Burgos-Morón E, Pérez-Guerrero C, López-Lázaro M. A review on the dietary flavonoid kaempferol. Mini Rev Med Chem. 2011;11(4):298-344. doi:10.2174/138955711795305335
26. Devi KP, Malar DS, Nabavi SF, Sureda A, Xiao J, Nabavi SM, et al. Kaempferol and inflammation: from chemistry to medicine. Pharmacol Res. 2015;99:1-10. doi:10.1016/j.phrs.2015.05.002
27. Imran M, Rauf A, Shah ZA, Saeed F, Imran A, Arshad MU, et al. Chemo-preventive and therapeutic effect of the dietary flavonoid kaempferol: a comprehensive review. Phytother Res. 2019;33(2):263-75. doi:10.1002/ptr.6227
28. Gong JH, Shin D, Han SY, Park SH, Kang MK, Kim JL, et al. Blockade of airway inflammation by kaempferol via disturbing Tyk-STAT signaling in airway epithelial cells and in asthmatic mice. Evid Based Complement Alternat Med. 2013;2013:250725. doi:10.1155/2013/250725
29. Zhang J, Hong Y, Liuyang Z, Li H, Jiang Z, Tao J, et al. [Retracted] Quercetin prevents radiation-induced oral mucositis by upregulating BMI-1. Oxid Med Cell Longev. 2021;2021(1):2231680.
30. Lotfi M, Kazemi S, Ebrahimpour A, Shirafkan F, Pirzadeh M, Hosseini M, et al. Protective effect of quercetin nanoemulsion on 5-Fluorouracil-Induced oral mucositis in mice. J Oncol. 2021;2021(1):5598230.
31. Aziz N, Kim MY, Cho JY. Anti-inflammatory effects of luteolin: a review of in vitro, in vivo, and in silico studies. J Ethnopharmacol. 2018;225:342–58. doi:10.1016/j.jep.2018.05.019

32. Wang S, Cao M, Xu S, Shi J, Mao X, Yao X, et al. Luteolin Alters Macrophage Polarization to Inhibit Inflammation. Inflammation. 2020 Feb;43(1):95-108. doi:10.1007/s10753-019-01099-7
33. Reuter S, Gupta SC, Chaturvedi MM, et al. Oxidative stress, inflammation, and cancer: how are they linked? Free Radic Biol Med. 2010;49(11):1603–16. doi:10.1016/j.freeradbiomed.2010.09.006
34. Kao TI, Chen PJ, Wang YH, Tseng HH, Chang SH, Wu TS, et al. Bletinib ameliorates neutrophilic inflammation and lung injury by inhibiting Src family kinase phosphorylation and activity. Br J Pharmacol. 2021;178(20):4069-84. doi:10.1111/bph.15597
35. Zhang H, Huang J, Fan X, Miao R, Wang Y. HSP90AA1 promotes the inflammation in human gingival fibroblasts induced by Porphyromonas gingivalis lipopolysaccharide via regulating of autophagy. BMC Oral Health. 2022;22(1):366. doi:10.1186/s12903-022-02304-0
36. Li F, Song X, Su G, Wang Y, Wang Z, Qing S, et al. AT-533, a Hsp90 inhibitor, attenuates HSV-1-induced inflammation. Biochem Pharmacol. 2019;166:82-92. doi:10.1016/j.bcp.2019.05.003
37. Watanabe A, Yamamoto K, Ioroi T, Hirata S, Harada K, Miyake H, et al. Association of single nucleotide polymorphisms in STAT3, ABCB1, and ABCG2 with stomatitis in Patients with metastatic renal cell carcinoma treated with sunitinib: a retrospective analysis in japanese patients. Biol Pharm Bull. 2017;40(4):458-64. doi:10.1248/bpb.b16-00875
38. Bendix I, Pfueller CF, Leuenberger T, Glezeva N, Siffrin V, Müller Y, et al. MAPK3 deficiency drives autoimmunity via DC arming. Eur J Immunol. 2010;40(5):1486-95. doi:10.1002/eji.200939930
39. Kovats S. Estrogen receptors regulate innate immune cells and signaling pathways. Cell Immunol. 2015;294(2):63–9. doi:10.1016/j.cellimm.2015.01.018
40. Feng CJ, Guo JB, Jiang HW, Zhu SX, Li CY, Cheng B, et al. Spatio-temporal localization of HIF-1alpha and COX-2 during irradiation-induced oral mucositis in a rat model system. Int J Radiat Biol. 2008;84(1):35-45. doi:10.1080/09553000701616080
41. Firmal P, Shah VK, Chattopadhyay S. Insight into TLR4-mediated immunomodulation in normal pregnancy and related disorders. Front Immunol. 2020;11:807. doi:10.3389/fimmu.2020.00807
42. Ji L, Hao S, Wang J, et al. Roles of Toll-like receptors in radiotherapy- and chemotherapy-induced oral mucositis: a concise review. Front Cell Infect Microbiol. 2022;12:831387. doi:10.3389/fcimb.2022.831387
43. Saxton RA, Sabatini DM. mTOR signaling in growth, metabolism, and disease. Cell. 2017;168(6):960–76. doi:10.1016/j.cell.2017.02.004
44. Cosin-Roger J, Simmen S, Melhem H, Atrott K, Frey-Wagner I, Hausmann M, et al. Hypoxia ameliorates intestinal inflammation through NLRP3/mTOR downregulation and autophagy activation. Nat Commun. 2017;8(1):98. doi:10.1038/s41467-017-00213-3
45. Charbaji N, Rosenthal P, Schäfer-Korting M, Küchler S. Cytoprotective effects of opioids on irradiated oral epithelial cells. Wound Repair Regen. 2013;21(6):883-9. doi:10.1111/wrr.12115
46. Du L, Chen X, Cao Y, Lu L, Zhang F, Bornstein S, et al. Overexpression of PIK3CA in murine head and neck epithelium drives tumor invasion and metastasis through PDK1 and enhanced TGFβ signaling. Oncogene. 2016;35(35):4641-52. doi:10.1038/onc.2016.1